

Duplication and segregation of the actin (MreB) cytoskeleton during the prokaryotic cell cycle

Purva Vats and Lawrence Rothfield*

Department of Molecular, Microbial, and Structural Biology, University of Connecticut Health Center, Farmington, CT 06030

Communicated by M. J. Osborn, University of Connecticut Health Center, Farmington, CT, September 14, 2007 (received for review July 11, 2007)

The bacterial actin homolog MreB exists as a single-copy helical cytoskeletal structure that extends between the two poles of rod-shaped bacteria. In this study, we show that equipartition of the MreB cytoskeleton into daughter cells is accomplished by division and segregation of the helical MreB array into two equivalent structures located in opposite halves of the predivisional cell. This process ensures that each daughter cell inherits one copy of the MreB cytoskeleton. The process is triggered by the membrane association of the FtsZ cell division protein. The cytoskeletal division and segregation events occur before and independently of cytokinesis and involve specialized MreB structures that appear to be intermediates in this process.

septasome | FtsZ | cell division

Rod-shaped bacteria such as *Escherichia coli* contain a cytoskeletal element, composed of the actin homolog MreB (1), that extends along the length of the cell as a membrane-associated helical structure (Fig. 1 *A-i* and *A-ii*) (2–7). The MreB cytoskeleton has been implicated in several cellular processes, including chromosome segregation, regulation of cell shape, and determination of cell polarity (reviewed in ref. 7).

During the division cycle, cellular elements that exist as single-copy structures, such as these (Fig. 1 *A-i* and *A-ii* and figure 4*L* of ref. 3), must either be duplicated and segregated before completion of cytokinesis or assembled *de novo* in the progeny cell to ensure that each daughter cell receives a single copy of the cellular element. In the only well studied example of this process, individual chromosomes are duplicated by a template-directed mechanism and then moved to opposite ends of the cell by mechanisms involving microtubules in eukaryotic cells (8) or actin homologs in the case of some unit-copy bacterial plasmids (9–11). We report here that the actin (MreB) cytoskeleton of *E. coli* is also duplicated and segregated before cell division, ensuring the equipartition of the cytoskeletal element into the two daughter cells.

In addition to its characteristic helical organization in most cells of actively growing cultures (Fig. 1 *A-i* and *A-ii*), MreB is present in some cells as a transverse band or ring that extends across the cell cylinder (Fig. 1 *B-i* and *B-ii*) and is often, but not always, located near midcell (2–5, 12). The function of the MreB rings is not known.

In the present study, we show that the helical MreB cytoskeletal element that exists during most of the cell cycle is split into two equivalent structures in a process that is triggered by the membrane association of the FtsZ cell division protein. The transverse MreB ring structures appear to be intermediates in this process. This process is followed by segregation of the new cytoskeletal structures within the predivisional cell, leading to their equal partition into daughter cells when cytokinesis takes place.

Results

Organization of MreB. Fluorescence localization studies of Yfp-MreB in *E. coli* confirmed previous reports (3, 13) that MreB is organized in most cells as a filamentous element that coils around the *E. coli* cell, forming a double-helical structure along

its long axis (Fig. 1 *A-i* and *A-ii*). In addition, as described (3), some cells contained transverse Yfp-MreB bands that extended across the cell cylinder (Fig. 1 *B-i* and *B-ii*). The bands sometime appeared as paired dots on opposite sides of the cylinder (arrowheads in Fig. 1*E-i*), suggesting an annular structure. The MreB bands were usually positioned near the center of the cell (Fig. 1 *B-i*) although some cells contained bands close to a cell pole (Fig. 1 *B-ii*). Immunofluorescence microscopy of WT cells, using anti-MreB antibody, showed a similar pattern of helical structures and bands (Fig. 1 *C* and *D*), confirming that they were not artifacts of Yfp labeling. The relatively small number of labeled cells with MreB bands [$\approx 1\%$ in this study and 5% in a previous study (3)] suggested that the bands might be present transiently during the cell cycle.

MreB bands were also present in nonseptate filamentous cells induced by treatment with aztreonam, a specific inhibitor of the essential septation protein PBP3 (FtsI) (14, 15). The filaments contained multiple MreB bands that were often positioned at approximately regular intervals of 2–3 μm along the cell cylinder, as shown by Yfp-MreB fluorescence (Fig. 1 *E-i* and *E-ii*) and anti-MreB immunofluorescence microscopy (Fig. 1 *F-i*).

In cells containing MreB bands, less intense coiled structures were present along the remainder of the cell (Fig. 1 *E-i* and *I*). Thus, the pole-to-pole helical MreB structure did not disappear when the bands were formed, although its intensity was reduced, sometimes making it difficult to clearly see the details in low-contrast micrographs. The helical structures and bands in the aztreonam filaments resembled those seen in normally growing cells (see above). The number of MreB bands was much greater in the filaments than in dividing cells (≈ 0.4 and 7 bands per 100- μm cell length in untreated cells and aztreonam-induced filaments, respectively). The presence of MreB bands in the aztreonam filaments facilitated the analysis of events that occurred before septation, without the complications introduced by septal ingrowth and daughter cell separation.

Interestingly, the MreB bands were present both as single bands (singlets) (Fig. 1 *B-i*, *B-ii*, *D*, and *G-i*) and paired bands (doublets) (Fig. 1 *E-ii*, *F-ii*, *G-ii*, *K*, *L*, and *M*) in both WT cells (Fig. 1 *B-i*, *B-ii*, *D*, *G-i*, and *G-ii*) and aztreonam filaments (Fig. 1 *K-M*). The doublets were not caused by Yfp-MreB overexpression because they were also observed in anti-MreB immunofluorescence micrographs of WT cells (Fig. 1 *F-ii*). The ratio of MreB doublets to singlets was $\approx 1:4$ in the 200 filaments examined. 3D reconstruction of optically sectioned cells suggested that the MreB bands were circumferential ring structures that extended around the cell cylinder (Fig. 1*H*).

The 2D images and 3D reconstructions (Fig. 1 *I* and *J*) suggested that the MreB ring may form a bridge between the two

Author contributions: P.V. and L.R. designed research; P.V. performed research; P.V. and L.R. analyzed data; and P.V. and L.R. wrote the paper.

The authors declare no conflict of interest.

Abbreviations: IPTG, isopropyl β -D-thiogalactoside; LB, L-broth; PBS-T, PBS containing 0.02% Tween 80.

*To whom correspondence should be addressed. E-mail: lroth@neuron.uconn.edu.

© 2007 by The National Academy of Sciences of the USA

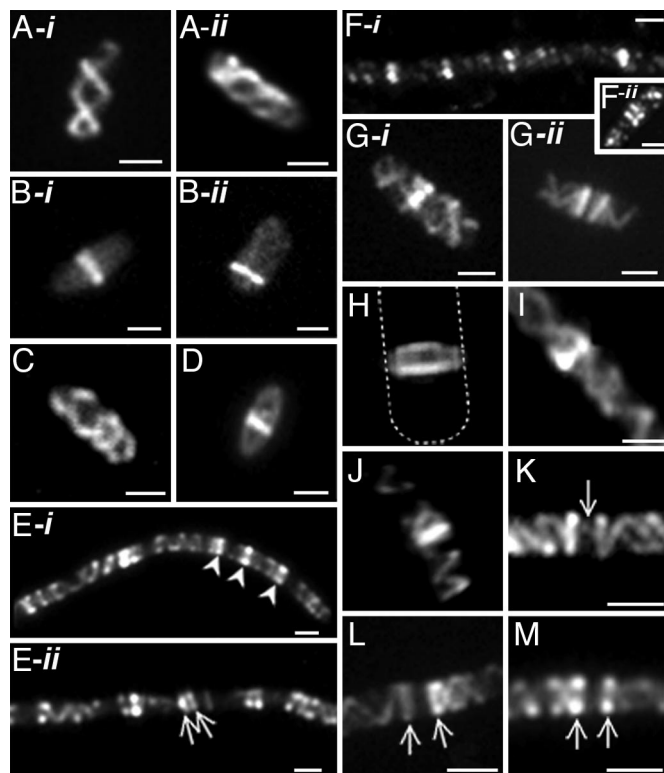


Fig. 1. Organization of MreB in *E. coli*. Cells were grown in the absence (MC1000) or presence (MC1000/pLE7 [wt/*Plac-yfp::mreB*]) of IPTG (see *Materials and Methods*). (A-i, A-ii, B-i, and B-ii) Fluorescence images of Yfp-MreB in MC1000/pLE7. (A-i and A-ii) Double-helical MreB cytoskeletal structure. (B-i and B-ii) MreB bands near midcell (B-i) and cell pole (B-ii). (C and D) Immunofluorescence images of MC1000 stained with anti-MreB antibody, showing MreB helical structure (C) and MreB band (D). (E-i, E-ii, F-i, and F-ii) MreB localization in nonseptate filaments of aztreonam-treated *E. coli* cells by Yfp-MreB fluorescence in MC1000/pLE7 (singlets indicated by arrowheads in E-i, and doublets by arrows in E-ii) and immunofluorescence in MC1000 cells using anti-MreB antibody (F-i and F-ii). (G-i and G-ii) Yfp-MreB localization in MC1000/pLE7 showing singlet (G-i) and doublet MreB bands (G-ii). (H-J) 2D image (I) and 3D reconstructions (H and J) of Yfp-MreB distribution in optically sectioned aztreonam-treated MC1000/pLE7 cells showing the ring-like structure of an MreB band (the dashed line shows the outline of the vertically oriented cell, from a higher contrast image of the micrograph) (H) and the relationship of MreB bands to the MreB helical structure (I and J). (K) Yfp-MreB localization in a nonseptate filament of aztreonam-treated MC1000/pLE7 showing a faint MreB strand (arrow) between the two bands of a MreB doublet. (L and M) Yfp-MreB localization in nonseptate filaments of aztreonam-treated MC1000/pLE7. The images show an attachment of the helical structures to the two rings of MreB doublets. (Scale bars: 1 μm .)

strands of the MreB double helix. The appearance of the “bridge” structures was similar in normal cells (Fig. 1 G-i) and aztreonam-induced filaments (Fig. 1 I and J). Similar results were obtained in immunofluorescence experiments (data not shown).

Relation of MreB Rings to Cytoskeletal Division. Evidence that the MreB rings are associated with splitting of the single MreB helical cytoskeleton into two structures came from time-lapse studies of Yfp-MreB labeled cells enrobed in agar, where they grow more slowly than in liquid medium.

The first detectable event was the formation of a single MreB band oriented at right angles to the continuous MreB helical array (Fig. 2A). The helical MreB structure remained in place during and after the formation of the MreB singlets. Double-label studies of WT cells (Fig. 3A) and aztreonam filaments (Fig. 3 C and E) showed that the single MreB rings were located

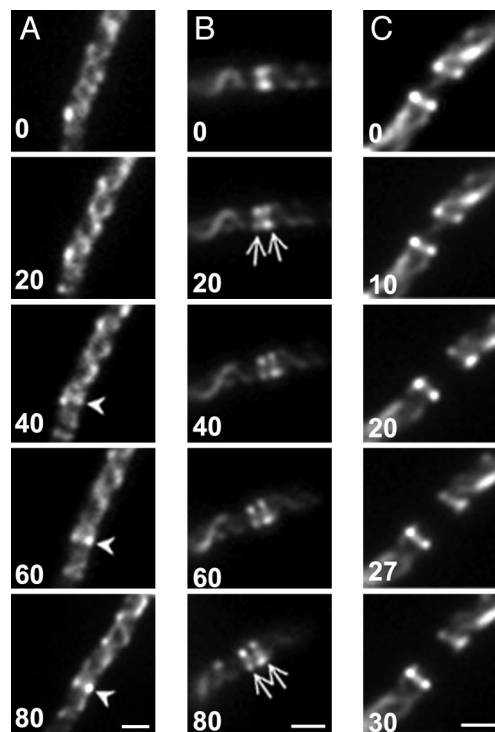


Fig. 2. Genesis of MreB singlets and doublets. Time-lapse images of MC1000/pLE7 cells grown in the presence of IPTG and aztreonam. Cells were transferred to soft agar slides containing 1 μM IPTG and 0.5 $\mu\text{g/ml}$ aztreonam. Numbers indicate time in minutes from the first selected time point. (A) Formation of a single MreB ring (arrowhead) within a helical array. (B) Splitting of single MreB ring into two rings (arrows). (C) Disappearance of MreB strand between MreB doublet rings. (Scale bars: 1 μm .)

adjacent to the FtsZ ring (Z-ring) that marks the future septation site in WT cells (16, 17) and the potential division sites of nonseptate filaments (18). We saw no instances where the MreB singlet bands and FtsZ rings were present at the same position but cannot exclude the possibility that the MreB and FtsZ structures were colocalized transiently at an early stage of formation of the MreB singlet.

Formation of the singlet was followed by the appearance of a second MreB ring immediately adjacent to the original single ring, giving rise to the MreB doublet. The two rings then moved apart to form the mature doublet structure (Fig. 2B). Double-label fluorescence microscopy of WT cells (Fig. 3B) and aztreonam filaments (Fig. 3 D and E) showed that the individual rings of the MreB doublet were located on opposite sides of the FtsZ ring, thereby flanking the potential division site.

Strikingly, appearance of the MreB doublet was accompanied by disappearance of the MreB helical structure between the two MreB rings (Figs. 1 L and M, 2C, and 3D). The disappearance of the connecting MreB strand interrupted the pole-to-pole coiled array, thereby splitting the helical MreB cytoskeleton into two halves, with one MreB coiled structure extending laterally from each of the paired MreB rings (Fig. 3D). The rings remained as caps at the ends of the two newly formed MreB helical structures (Figs. 1 L and M and 3D). As a result, in WT cells the two helical structures were located in opposite halves of the cell (Fig. 1G-ii).

Between the bands of a doublet, a faint MreB strand was sometimes visible that disappeared during the time course of observation (Figs. 1K and 2C, 0 min). This finding suggested that cleavage of the helical structure might be initiated or completed after doublet assembly.

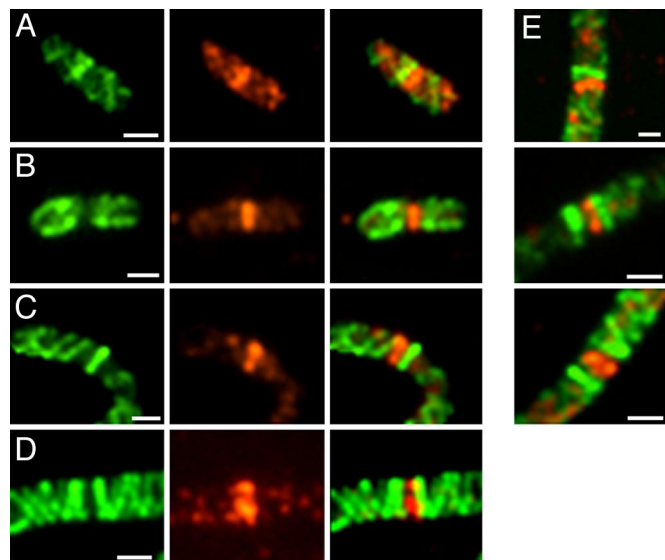


Fig. 3. Double-label staining of MreB and FtsZ in MC1000/pLE7. (A and B) MreB localization in cells without aztreonam. (C and D) After aztreonam treatment. Green indicates Yfp-MreB fluorescence (Left); red indicates anti-FtsZ immunofluorescence (Center). (Right) Overlays of the other two images. (E) Aztreonam-treated cells with MreB singlet and doublet rings flanking FtsZ ring. (Scale bars: 1 μm .)

Segregation of MreB Cytoskeleton. After the doublet was formed, the two closely spaced rings moved apart (Figs. 2B and 4A). The division septum then invaginated into the MreB-free zone between the two MreB rings (Nomarski and fluorescence images in Fig. 4A). Septation between the MreB doublet rings was observed in normally dividing WT cells (Fig. 4C) and when septation was permitted to resume by washing out the drug in aztreonam-induced filaments (Fig. 4A). When septation was completed, MreB rings often remained at the new poles of the postdivision cell (Fig. 4A and C), presumably explaining the observation that some cells in random cultures contained an MreB ring at one cell pole, representing the new pole of a postdivision cell (Fig. 1B-ii). The polar rings then disappeared (Fig. 4B), leaving the bright pole-to-pole helical array that is characteristic of most cells in exponentially growing cultures (Fig. 1A-i and A-ii).

Relation of MreB Rings to the Division Apparatus. Formation of the bacterial division septum is preceded by assembly of a multi-protein septasome complex that is visible as a ring extending around the cell cylinder at the division site (16, 19). The septasome is required for invagination of the division septum and subsequent separation of the daughter cells. In *E. coli*, the septasomal ring includes at least 11 proteins that are incorporated in an ordered sequence (Fig. 5A) (20, 21). In the first known step in this sequence, FtsZ assembles into an annular structure (the Z-ring) that is thought to act as a scaffold for subsequent introduction of the other septasomal proteins (7, 22).

Evidence that assembly of the MreB ring requires the function of one or more components of the septasomal complex came from studies of FtsZ depletion and repletion in strain WX7/ λ GL100 [Δ ftsZ/*P_{lac}-ftsZ*], where septasome assembly and septum formation depend on induction of FtsZ. FtsZ was depleted by growth in the presence of glucose, leading to formation of nonseptate filaments that lack Z-rings (Fig. 5B-i). Strikingly, immunofluorescence experiments revealed that MreB rings were virtually absent in the FtsZ-depleted filaments (Fig. 5B-ii). This was accompanied by the presence of a prominent helical MreB array extending along the long axis of the cell (Fig. 5B-ii).

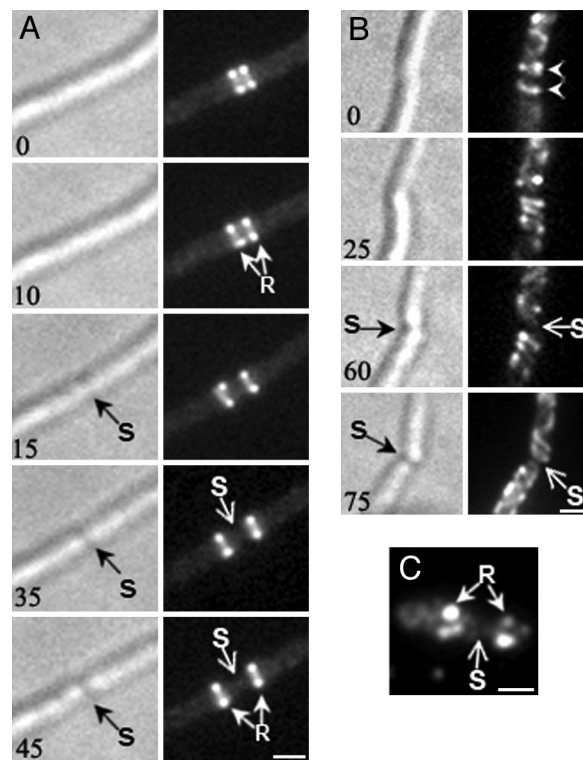


Fig. 4. Relation of MreB rings to site of septation after aztreonam removal. MC1000/pLE7 cells were treated with aztreonam for 90 min. The drug was then removed by centrifugation and washing with LB medium before transferring the cells to soft agar slides containing 1 μM IPTG for time-lapse study. Numbers indicate time in minutes from the first selected time point. (A) Separation of the MreB doublet rings followed by in-growth of the division septum (S) between the two rings (R). (B) Septal in-growth (S) followed by disappearance of the MreB doublet bands (arrowheads). (C) Anti-MreB immunofluorescence micrograph of septating WT MC1000 cell. MreB rings (R) are present on both sides of septum (S) corresponding to the newly forming cell poles. (Scale bars: 1 μm .)

The absence of MreB rings in FtsZ-deficient cells has also been described in *Caulobacter crescentus* (4). Quantitative immunoblot analysis confirmed that the cellular concentration of MreB was essentially unaffected under these conditions, in which FtsZ concentration was reduced \approx 20-fold (data not shown).

In contrast to the effects of FtsZ depletion, inactivation of the late-appearing septasomal component FtsI by treatment with aztreonam did not prevent the formation of MreB rings, as shown above (Fig. 1E-i, E-ii, F-i, and F-ii). Similarly, inactivation of FtsQ, an early participant in septasome assembly, in a temperature-sensitive *ftsQ(ts)* mutant, also failed to prevent the appearance of MreB rings, which were present at 5- to 6- μm intervals along the length of the FtsQ⁻ filaments (Fig. 5C-ii). The FtsQ⁻ filaments contained Z-rings (Fig. 5C-i) at potential division sites along the length of the filaments as reported (16).

The presence of MreB rings in FtsI⁻ (aztreonam treated) and FtsQ⁻ cells and their absence in FtsZ⁻ filaments implies that MreB ring assembly requires a component whose entry into the septasomal ring occurs early in septasome assembly, before the entry of FtsQ (Fig. 5A).

The role of septasome assembly in MreB ring formation was further investigated by the study of septasomal proteins FtsA and ZipA. FtsA and ZipA are each individually capable of supporting FtsZ membrane association and Z-ring formation, although both proteins must normally be present for incorporation of the other septasomal proteins (23). Inactivation of FtsA or depletion of ZipA by growth of strains WC1006 and CH5/pCH32 under

and one of the two FtsZ membrane-anchoring components, FtsA or ZipA, under conditions where the other septosomal components fail to enter the septosomal ring. Z-rings also reappeared before appearance of new MreB rings in FtsZ depletion–repletion experiments, supporting the view that the Z-ring plays a causal role in MreB ring assembly, rather than the alternative model in which the two ring structures are coordinately coassembled.

It has previously been shown that in *C. crescentus* MreB localized in a band structure at the future division site at a time that coincided with the initiation of cell division (4, 5) and that depletion of FtsZ was associated with disappearance of the MreB bands (4). This finding suggests that the FtsZ dependence of MreB ring assembly represents a general mechanism in rod-shaped bacteria, although it was not established whether the loss of MreB rings in *C. crescentus* was caused by the loss of FtsZ, the resulting absence of other septosomal components, or the absence of cytokinesis itself. The mechanism responsible for the effect of the Z-ring on MreB redistribution and ring formation remains to be elucidated.

The significant decrease in intensity of the pole-to-pole MreB helical array that accompanies the appearance of MreB rings (Fig. 5 *B–E* and *Gii*) suggests that the ring is assembled by recruiting molecules from the preexisting helical cytoskeleton. It is not known whether this recruitment occurs by MreB release and recapture from the cytoplasm or whether MreB molecules move translationally along the helical elements to form the MreB ring structures.

(iii) The MreB singlet ring is converted to an MreB doublet that flanks the Z-ring (stage 3). The details of the singlet–doublet conversion and the relation of the MreB rings to the Z-ring during the conversion have not yet been resolved. Because the doublet is first visible as a pair of closely apposed individual rings that then move apart, it is possible that the MreB “singlet” ring may be a tightly packed doublet. The only other known paired structures that flank the division site are the continuous zones of adhesion (periseptal annuli) between inner membrane and the murein-outer membrane layer that have been reported to extend partially or completely around the cell cylinder on either side of the division site (24, 25). It is not known whether there is a relationship between these structures and the MreB doublet elements.

(iv) The continuity of the MreB helical cytoskeleton is interrupted between the rings of the MreB doublet (Fig. 6 *A*, stages 3 and 4, *Bii*, and *Biii*). This interruption divides the pole-to-pole MreB coiled array into two halves. The cytoskeletal division event presumably involves two processes that are tightly coupled. It is likely that the MreB rings play a role in one or both of these events. In the first step, the linear continuity of the cytoskeletal structure must be interrupted (Fig. 6*Bii*), which presumably requires the localized cleavage of MreB polymers or the breaking of interactions between shorter MreB polymeric units if the helical array is composed of multiple short MreB segments. A component associated with the rings could play a direct role in this process, although it cannot be excluded that other elements at the future division site may be responsible for this event. In the second step, the newly generated ends must be prevented from resealing to avoid reconstitution of the original pole-to-pole structure. The fact that the MreB doublet rings remain at the ends of the two new helical arrays leads us to suggest that an important role of the MreB rings is to cap and stabilize the ends of the new structures (Fig. 6*Biii*), thereby preventing the non-productive regeneration of the original MreB cytoskeletal element. The cleavage and capping events may involve an intermediate structure in which the MreB ring first intercalates as a bridge between the two helical strands (Fig. 6*Bii*). After cleavage, the MreB rings would then remain as the terminal loops of the two new helical structures (Fig. 6*Biii*). The fluorescence

images are consistent with this mechanism but the resolution of the method is insufficient to definitively identify the proposed intermediates. Although shown here as occurring after formation of the MreB doublets, the cleavage and capping events could occur before separation of the MreB singlet into the two rings of the doublet.

(v) The two rings of the MreB doublet move progressively farther apart (Fig. 6*A*, stage 4), which pushes the two new cytoskeletal structures toward opposite ends of the cell, thereby segregating them in preparation for cell division. The septum then grows inward within the cytoskeleton-free space that lies between the paired MreB rings.

(vi) The rings disappear because of movement of molecules from the MreB caps into the extended helical MreB structures during or after septation. Interestingly, the number of MreB singlets and doublets along the cell cylinder, expressed as number of singlets and doublets per unit cell length, was ≈ 30 -fold higher in nonseptating filaments blocked at intermediate stages of septosome assembly than in unsynchronized WT cells. This result suggests that the filamentous cells may be defective in ring disassembly, implying that septation itself or some late event in septosome assembly could be the trigger for MreB ring disassembly.

Segregation of the MreB Cytoskeleton. The movement of the two products of the MreB division event toward opposite ends of the cell results in their segregation within the predivisional cell. We speculate that this process is driven by the insertion of new preseptal murein between the two rings that cap the cytoskeletal structures. It has been shown that a period of localized murein synthesis (“preseptal murein” synthesis) occurs at the future division site before septal ingrowth (26, 27). Preseptal murein synthesis requires FtsZ but is independent of cytokinesis and cell division (26). This finding is consistent with the idea that FtsZ or another septosomal component may play a direct role in synthesis of preseptal murein. However, the possibility should also be considered that the MreB rings, whose formation also depends on the FtsZ ring and is independent of cell division, might play a role in catalyzing preseptal murein synthesis. A role for MreB in murein synthesis along the length of growing cells has been inferred from the involvement of the helical MreB cytoskeleton in the spatial organization of murein synthetic factors during cell elongation (4, 28, 29). Redistribution of these factors to midcell by the MreB central rings could permit them to catalyze the localized synthesis of preseptal murein. Therefore, it will be of interest to learn whether murein biosynthetic proteins are associated with the MreB doublet rings that flank the future septation site. Of interest in this regard is the observation that PBP2, a murein biosynthetic enzyme, shows MreB-dependent localization at midcell (4).

Relationship of Cytoskeletal Division and Cell Division. Cytoskeletal division can be totally uncoupled from septal invagination and cell division. Thus, in the present study, assembly of the MreB rings and the division and segregation of the MreB helical arrays occurred even in cells that were unable to septate because of genetic blocks or aztreonam treatment. This observation excludes the possibility that the helical cytoskeleton is broken into two halves by the physical act of septal ingrowth. Formation of MreB rings in the absence of septation has also been shown in cephalixin-treated cells of *Rhodobacter sphaeroides* (12). These findings make it clear that duplication and segregation of the MreB cytoskeleton during the division cycle is independent of cell division itself.

E. coli cells also can septate and divide in the absence of MreB (13, 30, 31), provided that FtsZ levels are increased (30–32). This observation shows that neither the MreB ring structures nor the MreB cytoskeleton are required for cytokinesis. Together with

the present demonstration that the MreB rings are not positioned at the leading edge of the ingrowing septum, this finding excludes the possibility that the bacterial actin (MreB) ring acts as a contractile ring equivalent to the actin cytokinetic ring of eukaryotic cells. This conclusion is consistent with the demonstration that MreB ring structures near midcell in *R. sphaeroides* cells were present in predivisional cells but were not observed in septating cells (12).

We conclude that equal partition of the prokaryotic actin (MreB) cytoskeleton into daughter cells involves specific mechanisms of cytoskeletal division and segregation that are cell cycle-regulated and operate before and independently of the cytokinetic event that gives rise to the progeny cells. If the MreB rings include protein components, they could be responsible for important aspects of these events. The MreB rings may also play a direct or indirect role in other cellular processes, such as establishment of cell polarity (5).

Materials and Methods

Strains, Plasmids, and Growth Conditions. *E. coli* strains and plasmids (relevant genotypes in brackets) used were: MC1000 (3), WC1006 [*ftsA12(ts)*] (18), CH5/pCH32 [*zipA::aph/repA(ts) zipA⁺ ftsZ⁺*] (33), TOE1 [*ftsQ(ts)*] (34), WX7/ λ GL100 [Δ *ftsZ/P_{lac}-ftsZ*] (35), PS234 [W3110 *zipA1(ts) ftsA12(ts)*] (kindly provided by J. Lutkenhaus, University of Kansas, Kansas City, KS; ref. 23), and pLE7 [*P_{lac}-yfp::mreB*] (3). When plasmids were present, appropriate amounts of antibiotics were added. Where indicated, 1 μ g/ml aztreonam was added for 2 h to block septation.

CH5/pCH32 and TOE1 [in L-broth (LB) with no salt], WC1006 (in LB/0.4% NaCl), and PS234 (in LB) were grown at 30°C before shifting to 42°C for 2 h. Strains containing pLE7 were grown for 90–120 min at 37°C in the presence of 20 μ M IPTG.

For FtsZ depletion, WX7/ λ GL100 was grown at 37°C in LB containing 0.4% glucose for 4–6 h. For FtsZ repletion, cells were then resuspended in LB containing 20 μ M IPTG and incubated at 37°C.

Microscopy. Fluorescence microscopy, optical sectioning, deconvolution, and 3D reconstructions were performed as described (3).

For immunofluorescence microscopy, polyclonal blot-purified anti-MreB and affinity-purified anti-FtsA, anti-ZipA, and anti-FtsZ were used as primary antibodies. Cells were fixed in growth medium by using 1.6% formaldehyde and 0.01% glutaraldehyde

for 1 h at room temperature; similar results were obtained with fixation in 0.1 M phosphate buffer (pH 6.7). After washing with PBS-T (PBS containing 0.02% Tween 80) and Tris-glucose-EDTA buffer, the cells were permeabilized by treatment with lysozyme (5 μ g/ml) for 5 min at room temperature and then washed with PBS-T and applied to polylysine-treated coverslips for 1 h at room temperature. After washing with PBS-T and blocking overnight at 4°C with 2% BSA in PBS-T, the cells were treated with primary antibodies and Alexafluor 594 goat anti-rabbit IgG (Molecular Probes, Carlsbad, CA) diluted in the blocking solution for 4 h at room temperature. The coverslips were washed with PBS-T and mounted by using 2.5% 1,4-diazabicyclo[2.2.2]octane in 0.1 M Tris, pH 7.5. Fluorescence was observed with a Texas red filter cube (Chroma, Rockingham, VT).

For simultaneous localization of Yfp-MreB and FtsZ, MC1000/pLE7 was grown in the presence of IPTG (see above). Cells were fixed in the culture medium by using 1% formaldehyde and 0.01% glutaraldehyde for 1 h at room temperature and then permeabilized and stained with antibodies as described above. Cells were observed for FtsZ immunofluorescence by using a Texas red filter cube (Chroma) and for Yfp-MreB by using a YGFP filter cube (Chroma).

Time-Lapse Experiments. MC1000/pLE7 was grown in the presence of IPTG (see above). Cells were then mixed with LB soft agar containing 2 μ M IPTG, unless otherwise stated, to an Abs_{600nm} of 0.1 ($\approx 2 \times 10^8$ cells per ml). One microliter of the agar suspension was introduced into a well of a Multitest 12-well slide (MP Biomedicals, Aurora, OH), covered with a coverslip, and incubated at 34°C on a temperature-controlled stage. Fluorescence and Nomarski images were collected at 5- to 10-min intervals.

Immunoblot Analysis. Quantitative Western blot analysis was performed essentially as described (36) with an alkaline phosphatase-conjugated substrate kit (Bio-Rad, Hercules, CA). Polyclonal blot-purified anti-MreB and affinity-purified anti-FtsA (35), anti-ZipA (provided by P. de Boer, Case Western University, Cleveland, OH), and anti-FtsZ were used as primary antibodies.

This work was supported by National Institutes of Health Grant GM R37-06032.

- Van den Ent F, Amos L, Lowe J (2001) *Nature* 413:39–44.
- Jones L, Carballido-Lopez R, Errington J (2001) *Cell* 104:913–922.
- Shih Y-L, Le T, Rothfield L (2003) *Proc Natl Acad Sci USA* 100:7865–7870.
- Figge RM, Divakaruni AV, Gober JW (2004) *Mol Microbiol* 51:1321–1332.
- Gitai Z, Dye N, Shapiro L (2004) *Proc Natl Acad Sci USA* 101:8643–8648.
- Soufo HJD, Graumann PL (2004) *EMBO Rep* 5:789–794.
- Shih Y-L, Rothfield L (2006) *Microbiol Mol Biol Rev* 70:729–754.
- Alberts B, Johnson A, Lewis J, Raff M, Roberts K, Walter P (2002) *Molecular and Biological Cell* (Garland Science, New York).
- Kruse T, Gerdes K (2005) *Trends Cell Biol* 15:343–345.
- Gerdes K, Möller-Jensen J, Ebersbach G, Kruse T, Nordstrom K (2004) *Cell* 116:359–366.
- Soufo HJ, Graumann PL (2003) *Curr Biol* 13:1916–1920.
- Slovak PM, Wadhams GH, Armitage JP (2005) *J Bacteriol* 187:54–64.
- Kruse T, Möller-Jensen J, Lobner-Olesen A, Gerdes K (2003) *EMBO J* 22:5283–5292.
- Georgopapadakou NH, Smith SA, Sykes RB (1982) *Antimicrob Agents Chemother* 21:950–956.
- Den Blaauwen T, Aarsman ME, Vischer NO, Nanninga N (2003) *Mol Microbiol* 47:539–547.
- Addinall S, Bi E, Lutkenhaus J (1996) *J Bacteriol* 178:3877–3884.
- Ma X, Ehrhardt D, Margolin W (1996) *Proc Natl Acad Sci USA* 93:12998–13003.
- Cook W, Rothfield LI (1994) *Mol Microbiol* 14:497–503.
- Carballido-Lopez R, Errington J (2003) *Trends Cell Biol* 13:577–583.
- Aarsman ME, Piette A, Fraipont C, Vinkenvleugel TM, Nguyen-Disteche M, den Blaauwen T (2005) *Mol Microbiol* 55:1631–1645.
- Vicente M, Rico AI (2006) *Mol Microbiol* 61:5–8.
- Goehring NW, Beckwith J (2005) *Curr Biol* 15:R514–R526.
- Pichoff S, Lutkenhaus J (2002) *EMBO J* 21:685–693.
- MacAlister TJ, MacDonald B, Rothfield LI (1983) *Proc Natl Acad Sci USA* 80:1372–1376.
- Cook WR, Kepes F, Joseleau-Petit D, MacAlister TJ, Rothfield LI (1987) *Proc Natl Acad Sci USA* 84:7144–7148.
- de Pedro MA, Quintela JC, Holtje JV, Schwarz H (1997) *J Bacteriol* 179:2823–2834.
- Rothfield L (2003) *J Bacteriol* 185:1125–1127.
- Dye NA, Pincus Z, Theriot JA, Shapiro L, Gitai Z (2005) *Proc Natl Acad Sci USA* 102:18608–18613.
- Divakaruni AV, Loo RR, Xie Y, Loo JA, Gober JW (2005) *Proc Natl Acad Sci USA* 102:18602–18607.
- Kruse T, Bork-Jensen J, Gerdes K (2005) *Mol Microbiol* 55:78–89.
- Shih YL, Kawagishi I, Rothfield L (2005) *Mol Microbiol* 58:917–928.
- Varma A, de Pedro MA, Young KD (2007) *J Bacteriol* 189:5692–5704.
- Hale C, de Boer P (1997) *Cell* 88:175–185.
- Begg KJ, Hatfull GF, Donachie WD (1980) *J Bacteriol* 144:435–437.
- Justice SS, Garcia-Lara J, Rothfield L (2000) *Mol Microbiol* 37:410–423.
- Zhang Y, Rowland S, King G, Rothfield L (1998) *Mol Microbiol* 30:265–273.